J Solid State Electrochem (1998) 2: 137–145

ORIGINAL PAPER

Dominique Larcher · Bernard Gérand
Jean-Marie Tarascon

Synthesis and electrochemical performances of $Li_{1+y}Mn_{2-y}O_4$ powders of well-defined morphology

Received: 12 August 1997 / Accepted: 20 October 1997

Abstract The spinel phases $Li_{1+y}Mn_{2-y}O_4$ have been synthesized by a novel synthesis method that presents advantages compared to the classical ceramic method, namely, in terms of preparation time, costs and electrochemical performances of the resulting products. This consists of a two-stage process. First, two precursor phases (Li-EG and Mn-EG) are synthesized by reacting powdered lithium hydroxide and electrolytic manganese dioxide (EMD) in ethylene glycol (EG) under reflux, respectively. Secondly, the precursor products are mixed and heat treated under air, following various heating sequences, to produce electrochemically active $Li_{1+y}Mn_{2-y}O_4$ powders of well-defined morphology. Once the synthesis parameters involved in these two steps are controlled, the obtained $Li_{1+y}Mn_{2-y}O_4$ powders exhibit electrochemical performances that compare favorably with those observed in the case of the high-temperature (HT) $Li_{1+y}Mn_{2-y}O_4$ made by the ceramic route, both in terms of reversible/irreversible capacities and cycling behavior at 25 °C and 55 °C.

Key words Metal/organic precursors · Lithium manganese oxides · Lithium batteries · Polyol medium · Reaction mechanism

Introduction

Rechargeable Li-ion batteries are now well accepted in today's portable electronics. This commercial success has prompted intensive studies directed towards the search for better lithium intercalation compounds. Several approaches were centered either around (1) the search for new materials with greater capacities or (2) the improvement of existing ones, through chemical and physical means. The present work is related to the second approach and more specifically to the use of "soft chemistry" to prepare materials of well-defined and controlled morphology.

The layered $LiCoO_2$ and $LiNiO_2$ phases and the spinel compound $Li_{1+y}Mn_{2-y}O_4$ have been proposed as suitable high-voltage cathode materials for lithium-ion secondary batteries and have been intensively studied over the last decade [1]. If we compare these three suitable materials with regard to natural abundance, commercial cost, toxicity, recyclability and stability of their delithiated phases, the lithium manganese oxides $Li_{1+y}Mn_{2-y}O_4$ offer greater advantages relative to either $LiCoO_2$ or $LiNiO_2$. The spinel $Li_{1+y}Mn_{2-y}O_4$ is usually prepared in 15 days by reacting manganese oxide and lithium salt at 800 °C for a long period with intermittent cooling and grinding stages, and an extremely slow final cooling step [2]. From an industrial point of view, this process is slow and energetically expensive, and a novel route would be desirable. Many research efforts have been placed on studies and optimization of other synthesis processes erroneously regrouped under the name "sol-gel" [3–5]. The solution technique known as sol-gel consists of the condensation of metal-oxide networks from solution precursors. None of the solution techniques so far reported for $LiMn_2O_4$ synthesis has revealed, to our knowledge, the condensation of the spinel network from the solution. In all cases, the amorphous powders (e.g. xerogels) obtained from drying the gelatinous solution product always did need a post-annealing treatment at high temperatures to obtain the required phase. If these temperatures are usually slightly lower than those commonly used for the ceramic approach, this is only due to the fact that solution techniques in general (after drying of the solvent) produce xerogels with small grain size. Thus, upon heating of these

D. Larcher · B. Gérand · J.-M. Tarascon (✉)
Laboratoire de Réactivité et Chimie des Solides – UPRES-A 6007, Université de Picardie Jules Verne – 33, rue Saint-Leu, F-80039 Amiens Cedex, France

J.-M. Tarascon
Bellcore, NVC 3Z-281,
331 Newman Springs Road,
Red Bank, NJ 07701, USA

xerogels, the reduced diffusion path allows the phase to form at a lower annealing temperature. Despite their energetic advantages and the shorter preparation times involved, these solution techniques have not so far replaced solid-state reactions to prepare electrode materials. The reason is twofold: (1) the powders made following these routes have very small particle sizes (< 0.1 μm) and large surface areas, which are detrimental to their electrochemical behavior, and (2) the firing of organic compounds like acetates and tartrates makes it difficult for these methods to be accepted in industry.

We propose an alternative method of $Li_{1+y}Mn_{2-y}O_4$ preparation that can be described as a two-step process: (1) the synthesis of two crystallized organometallic precursors (Li-EG and Mn-EG) using the same reactants as those used in the ceramic process, and (2) the subsequent heating treatment of a stoichiometric mixture of the two precursors to obtain electrochemically active $Li_{1+y}Mn_{2-y}O_4$. This process involves a short treatment time at 800 °C (24 h) to obtain $Li_{1+y}Mn_{2-y}O_4$ powders with a specific surface area similar to that of ceramic-made powders, but with a completely different morphology. Moreover, this synthesis allows the preparation of large quantities of material and yields spinel phases showing electrochemical performances that compare well with HT-$Li_{1+y}Mn_{2-y}O_4$.

Experimental section

Li-EG and Mn-EG precursor phases are synthesized in a glass vessel equipped with both a refrigerating unit and a mechanical stirring unit to ensure constant reflux and constant vigorous mechanical agitation, respectively. Depending on the precursor synthesized, MOH (M = Li, Na, K) alkali hydroxide (Prolabo and Merck >96%) or a mixture of MOH/γ-MnO_2 EMD (IBA#15, Japan Metals & Chemical Co) is added to the cold polyol medium (Prolabo, reagents grade), and the heating rate is tuned to 1°/min. The reaction medium temperature is monitored by means of a temperature controller. The final temperature is tuned from 160 °C to the boiling temperature of the polyol used. This temperature is maintained from several hours to some days and the cooling rate is set to 1°/min until ambient temperature is reached.

The solid and liquid phases are separated by vacuum filtration, and the recovered solid phase is washed and dried under vacuum for several hours. The washing step consists in one mechanical stirring of the solid phase in pure liquid polyol and several stirrings in dried ethanol. The recovered solid phase is kept under primary vacuum to avoid degradation by exposure to moisture.

The alkali metal and manganese contents in the solid phases and organic liquid media were determined by atomic absorption (AA) using a Perkin-Elmer 3030 spectrophotometer. To perform such an analysis, the solid phases were dissolved in an $H_2O/H_2O_2/HNO_3$ (90/5/5 v/o) solution. Phase identification was carried out by means of X-ray diffractometers (Philips PW 1710/1729 and INEL CPS 120) using CuK_α radiation (λ = 1.5418 Å). Infrared spectra of solid and liquid phases were obtained at ambient temperature with a Nicolet 510 FT-IR spectrophotometer. For solid phase analysis, a few milligrams of powder were mixed with 200 mg of KBr dried at 125 °C, and pelletized at 8 t/cm^2. Infrared spectra of liquid phases were collected by placing a drop of the liquid to be studied between two KBr pellets. Scanning electron microscopy (SEM) images were obtained by means of Philips SEM 505 and Philips FEG XL-30 microscopes, TEM/SAED studies were conducted on a STEM CM12 Philips microscope, while EDS analyses were made by means of a Link Isis X-ray analyzer.

The manganese mean oxidation state (Mn o. s.) was obtained by the ferrous sulfate analytic method [6] that consists in reducing the $Mn^{2+\delta}$ to Mn^{2+} in an acidic solution of ferrous ammonium sulfate followed by a back titration of the non-consumed Fe^{2+} by a $KMnO_4$ solution. The calculated amount of Fe^{2+} consumed and the Mn weight percentage in the solid phase determined by AA are used to evaluate the mean oxidation state of the manganese. This method leads to an accuracy evaluated to +/− 0.02. Typically, ca. 0.5 g of sample is used for such an analysis.

Electrochemical tests were made in Swagelok TM cells. The $Li_{1+y}Mn_{2-y}O_4$ powders were dispersed into a plastic according to Bellcore PLiON technology [7]. The positive electrode plastic layer is made by mixing 56 parts by weight of lithium metal oxide powder and 6 parts by weight of carbon black (SP), and by intimately dispersing this mixture in a binder matrix of 15 parts of an 88 : 12 vinylidene fluoride : hexafluoropropylene (PVDF : HFP) copolymer (2801) plasticized with 23 parts of dibutylphthalate (DBP), to which the required amount of acetone is added to obtain a viscous paste. The resulting paste is spread on a glass substrate, the acetone evaporated and the resulting dried plastic layer cut into 1-cm^2 discs. Prior to being used as the positive electrode in the Swagelok cell, DBP is extracted by dried ether. Two sheets of Wattman GF/D borosilicate glass fiber, soaked with 1 M $LiPF_6$ in 2EC/DMC electrolyte, electrically separate $Li_{1+y}Mn_{2-y}O_4$ DBP extracted cathode discs from the lithium metal disc negative electrode. Cells were tested on a MacPile Macintosh controlled cycler (BioLogic Co., Claix, France) in a galvanostatic mode with a current charge/discharge stability better than 1%. Cycling data were collected at 25 °C and 55 °C between 3.5 V and 4.8 V at C/5 rate (one charge/discharge in 5 h).

Thermal analyses (TGA and DSC) were made using a Mettler apparatus under air flow (1 l/h) at a heating rate of 3 °C/min in a platinum crucible. Specific surface areas were measured with a Micromeritics (Norcross, Ga., USA) Gemini 2375 system according to the BET multi-point method [8] by nitrogen physisorption at 77 K. For typical measurements, prior to measuring the free space by means of helium gas, the samples were dried under argon flow at 110 °C for 1 h.

Results and discussion

Synthesis and characterization of the precursor phases

Mn-polyol

Synthesis and characterization. EMD (1.74 g 0.02 mole) is dispersed in 200 ml of cold ethylene glycol. To enhance the EG reducing power, the reaction is carried out in a highly basic environment obtained by adding an excess of LiOH to the polyol solution. Once the LiOH additive is totally dissolved, the suspension is heated under constant mechanical stirring while heating from ambient temperature to 196 °C at 1°/min. The first indication of an ongoing reaction is a change in the color of the suspension during the heating step. The initial black suspension quickly evolves to dark brown during the heating step and then, slowly, to pale pink when the final reaction temperature (196 °C) is reached. If not otherwise specified, the reactive medium is maintained at this temperature for several hours and then cooled down to ambient temperature at 1°/min. The obtained suspension is filtered to eliminate the reddish supernatant, and the recovered powder is washed following the

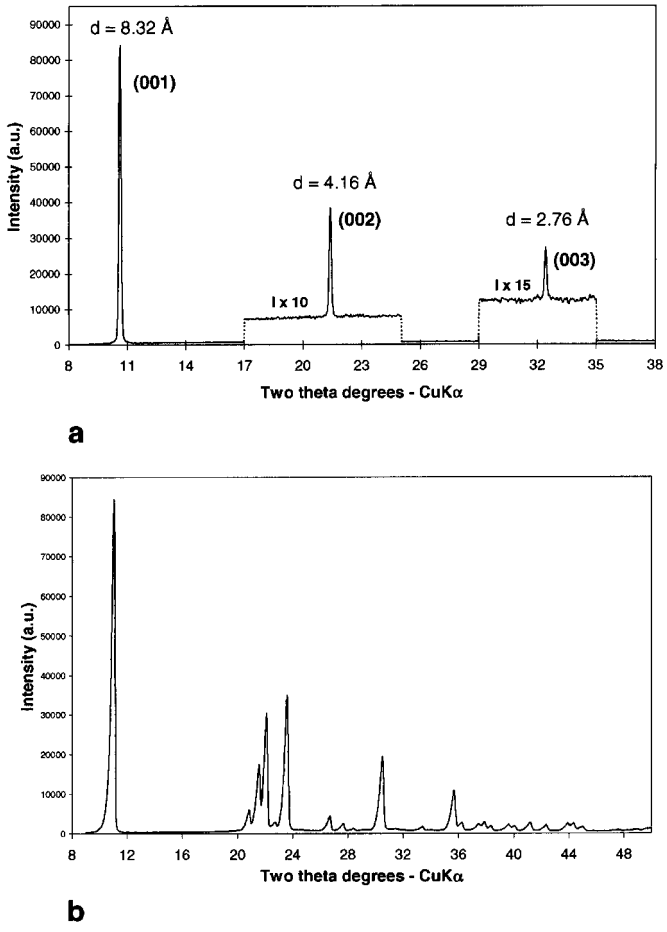

Fig. 1 **a** Typical XRD pattern of the Mn-EG precursor phase showing three peaks located at two theta degrees values of 10.63, 21.37 and 32.39 and corresponding to d-spacing of 8.32, 4.16 and 2.76 Å, respectively **b** Typical XRD pattern of Li-EG

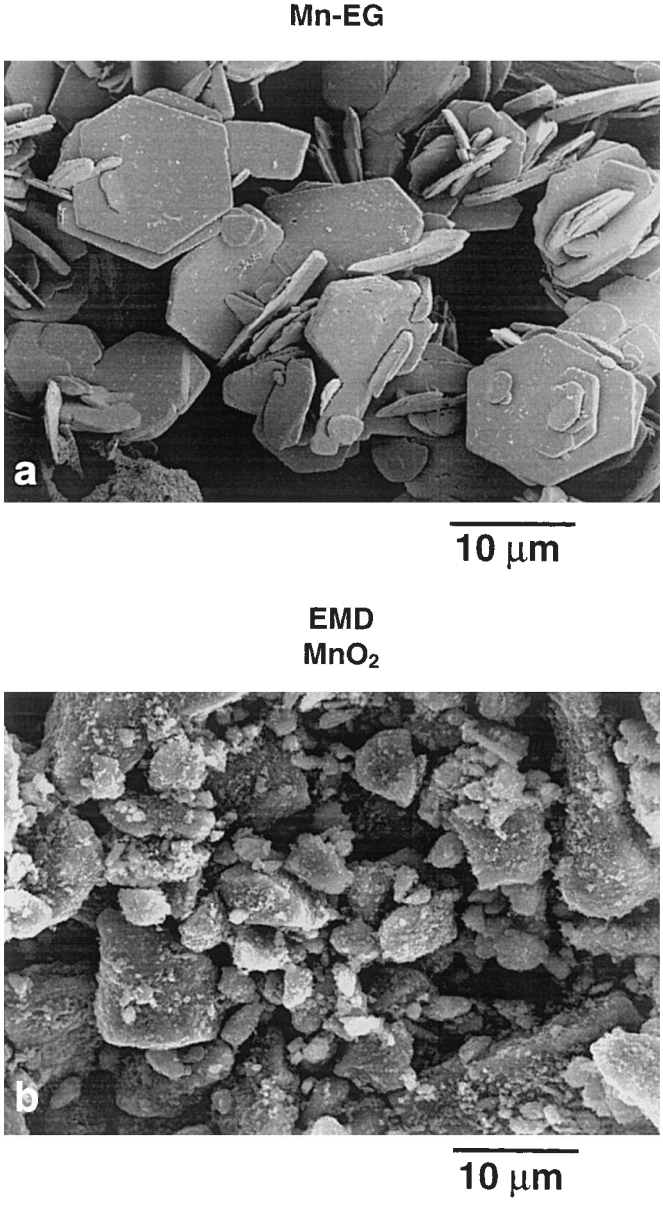

Fig. 2a, b SEM images showing the difference in morphology and size of **a** the final Mn-EG powder **b** EMD powder

sequence described in the experimental section. This Mn-EG powder, with a specific surface area of 2 m^2/g, is slightly colored and was found to be slightly unstable with respect to moisture, so it must be stored in dried air prior to be used.

The Mn-EG precursor exhibits an XRD pattern indicative of a highly preferentially oriented product, since we mainly observe 3 Bragg peaks (Fig. 1a). An SEM investigation of the Mn-EG product shows that it consists of particles that have a well-developed hexagonal shape (Fig. 2a) and are very large, with an average diameter of around 10 μm, thin, and twinned. TEM and electron diffraction (SAED) studies have been undertaken to collect information about the lattice type. A small hexagonal particle and its corresponding SAED pattern are shown in Fig. 3. This pattern clearly shows a hexagonal arrangement of the diffracted spots that fits perfectly with that simulated for an $Mn(OH)_2$ particle lying on the (001) plane. It is worth noting that the diffracted spots are not punctual but rather appear as slightly broad arcs, most likely related to disoriented crystallites within the particles. This hexagonal symmetry obviously indicates the presence of a sixfold axis perpendicular to the large hexagonal faces of the particle. Ongoing ED studies performed on larger platelets show, besides typical spots of the $Mn(OH)_2$ (001) plane, extra reflections that can be related to the presence of a super-structure. A complete crystallographic study by TEM/ED is actually in progress to confirm this superstructure, and to solve the structure of this lamellar compound [9]. From these results, we can guess that the structure, of our precursor consists of Mn-O layers stacked along the c sixfold axis. Such types of X-ray powder patterns are not unusual for low temperature prepared Mn-based phases, since similarly highly oriented powders mainly exhibiting the (00l) Bragg reflections have been previously reported for phyllo-

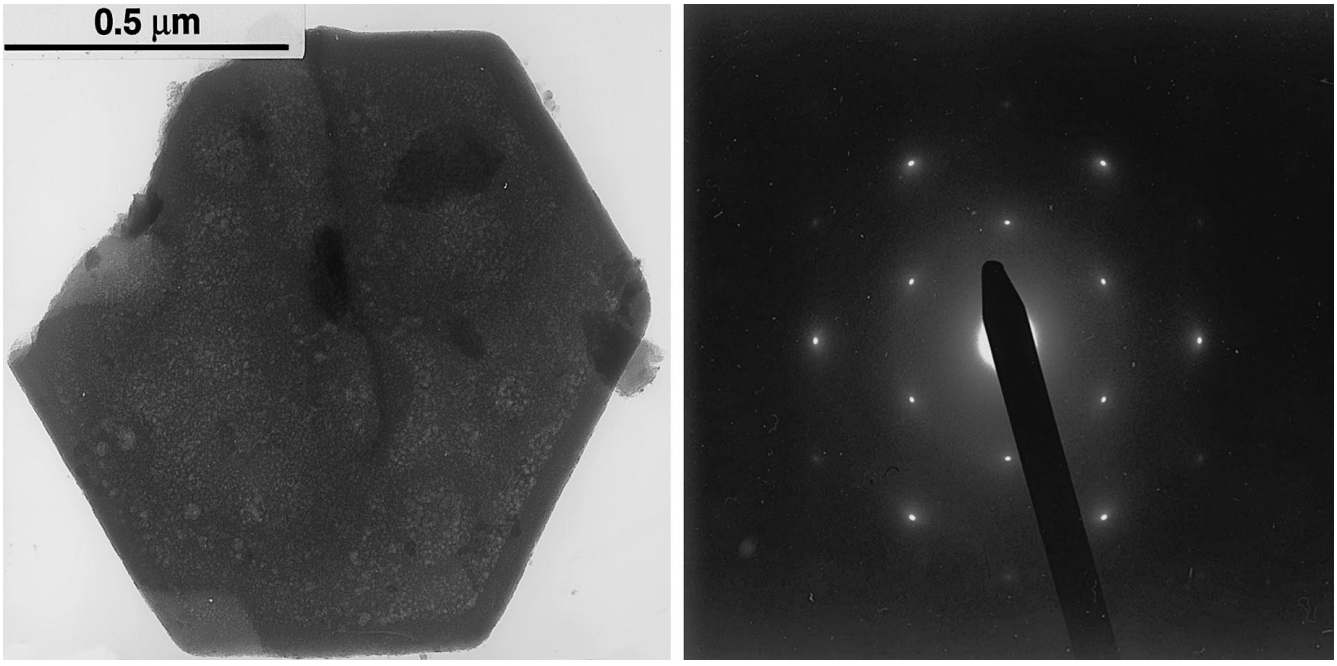

Fig. 3 Typical TEM image and SAED pattern on an Mn-EG particle

manganates with inserted water species between the Mn-O layers [10, 11].

A study of our Mn precursor by infrared spectroscopy (Fig. 4) reveals numerous absorption bands indicative of the presence of an organic phase in our precursor, most likely ethylene glycol. Attempts to remove this organic phase from our Mn-EG precursor by means of water treatments at 100 °C result in the formation of an EG-loaded surnatant and an organic free γ-Mn_2O_3 type phase ($MnO_{1.39} \cdot 0.53H_2O$) as determined by XRD, TGA and IR spectroscopy. A Mn-EG precursor heat-treated at 80 °C for 3 days under primary vacuum was found to exhibit the same XRD diffraction pattern, IR spectrum and TGA/DSC traces as those collected for the not heated precursor, implying that the IR bands are due to inserted rather than adsorbed ethylene glycol molecules in our particles. We can also note

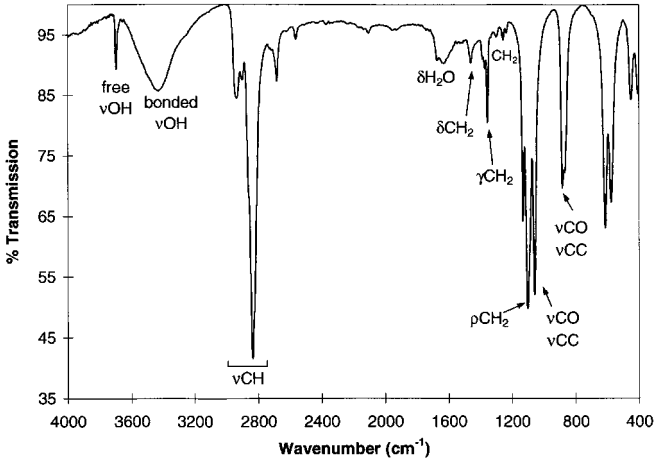

Fig. 4 Infrared spectrum of the Mn-EG phase

that the infrared spectrum for this phase is quite similar to that observed for nickel ethylene glycolate, which structure is described as nickel/oxygen layers with ethylene glycol molecules in between and shows an interlayer distance evaluated to be 8.31 Å [12, 13], very close to the 8.32 Å value deduced from the XRD pattern of Mn-EG. Finally, the presence of a narrow absorption band (3690 cm^{-1}) attributed to vibration of hydroxyl OH groups is not surprising if we bear in mind that such a layered hydroxide-type structure can contain some OH groups in the interlayer space. All these observations led to the conclusion that the Mn-EG phase contains ethylene glycol molecules between the Mn-O layers. Furthermore, interactions exist between these molecules and the Mn-O layers since the organic IR signature of the pure EG and that of the product containing EG show significant changes.

To check the influence of polyol medium on the structure of the Mn precursor, we fixed our experimental parameters (mass and ratio of components, heating and cooling rates, washing conditions) as before but changed the nature of the polyol used together with the reaction temperature, which is the boiling temperature of the polyol tested. The resulting precursor phases were characterized by XRD (Fig. 5). Table 1 summarizes the results of this survey. Close correlations can be noted between the (001) peaks position (e.g. intersheets distance) and (1) the organic molecule length of the polyol, (2) the number of OH groups, and (3) the OH groups position within the organic chain.

The different d-spacings for Mn precursors obtained using various polyol media confirm that the organic polyol molecules are present within the structure of the

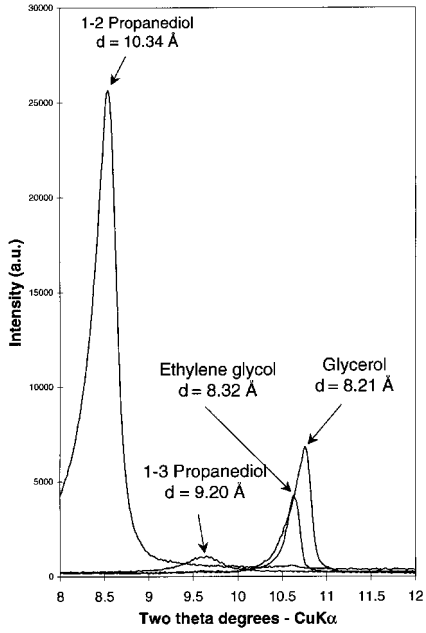

Fig. 5 Detailed XRD patterns of the Mn-based precursor phases prepared in various polyol media

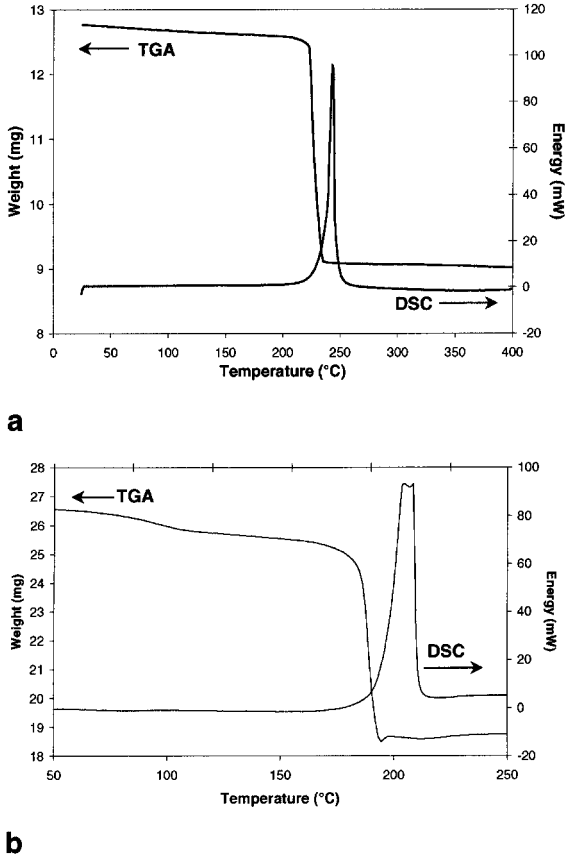

Fig. 6a, b Thermogravimetric (TGA) and calorimetric (DSC) curves for **a** the Mn-EG phase and **b** the Li-EG phase

Mn-polyol phases. The observed difference in the d-spacing could be explained by the steric effects of the organic molecules, steric effects, consistent with the inability to prepare pure Mn-polyol precursors when using a polyol having a molecular backbone longer than propanediol (3 carbon atoms). For instance, the experiments performed using 2-3- and 1-4-butanediol led to the layered $Mn(OH)_2$ type phase, which does not contain any organic component but large amounts of OH groups as determined by IR analysis.

TGA and DSC analyses of Mn-EG mainly show a strong exothermic effect associated with large weight loss around 240 °C (Fig. 6a) corresponding to the burning off of the organic. The final product at 800 °C is identified as well-crystallized α-Mn_2O_3. These results confirm that the precursor phase contains Mn together with an organic compound that burns below 250 °C. From the weight loss observed up to 800 °C, the calculation of the initial Mn content in the Mn-EG phase (47.07 wt% Mn) is consistent with a proposed formula $Mn(OCH_2CH_2O)_1$ (47.80 wt% Mn) in direct agreement with AA measurements (48.1 wt%). The small deviations from the theoretical formula arise from the presence of small quantities of adsorbed water and/or of small amounts of structural hydroxyl groups.

Reaction mechanism. How can such a lamellar structure and platelet morphology (Fig. 2a) be obtained for Mn-

Table 1 Variation of the d-spacing of the Mn-based precursor phases obtained with various polyol media

Polyol	Chemical formula	d_{001} (Å)
Ethylene glycol	**OH**—CH_2—CH_2—**OH**	8.32
Glycerin (Glycerol)	**OH**—CH_2—CH(**OH**)—CH_2—**OH**	8.21
1,2-Propanediol	CH_3—CH(**OH**)—CH_2—**OH**	10.34
1,3-Propanediol	**HO**—CH_2—CH_2—CH_2—**OH**	9.20
2,3-Butanediol	CH_3—CH(**OH**)—CH(**OH**)—CH_3	4.72 $Mn(OH)_2$
1,4-Butanediol	**HO**—CH_2—CH_2—CH_2—CH_2—**OH**	4.72 $Mn(OH)_2$
Diethylene glycol	**HO**—CH_2—CH_2—O—CH_2—CH_2—**OH**	/
Triethylene glycol	**OH**—$(CH_2)_2$—O—$(CH_2)_2$—O—$(CH_2)_2$—**OH**	/

EG when starting from EMD powders, which particles are very small, not well defined in shape, and strongly agglomerated (Fig. 2b)? The fact that the habitus is not preserved through the reaction implies that we are in the presence of a dissolution/crystallization process. As an attempt to better understand this reaction mechanism, we studied, by the use of sampling, the evolution of Mn and Li contents in the organic medium while the reaction proceeds. The reaction was first conducted in a single step at 196 °C and then in two steps to slow down the kinetics of the reaction and better follow its evolution. In the latter case, the temperature of the reaction was raised to 160 °C (1°/min), maintained for around 15 h, raised to 196 °C, maintained for 4 h and then cooled to ambient temperature. EMD (0.01 M) and LiOH (0.1 M) were reacted in 200 ml of EG, and each withdrawn sample (5 ml) was four times centrifuged to remove the remaining solid phases. The content of the surnatant in metallic elements is plotted versus time (Fig. 7) together with the temperature change through the reaction. The first unexpected result is that the Li content at the first stage of the reaction is not 0.1 M but only 0.085 M. Furthermore, it was found that this deviation from the initial content decreases with decreasing the amount of MnO_2 while maintaining the initial amount of LiOH constant. Secondly, our chemical analysis results successively indicate (1) a decrease of [Li] in the solution up to 125 °C while Mn begins to be detected in the solution above 80 °C, (2) a concomitant increase in both [Li] and [Mn] between 125 °C and 160 °C, (3) a decrease of [Mn] above 160 °C while [Li] increases to reach a final concentration of 0.1 M, and finally (4) a rapid increase of [Mn] while the temperature is reduced down to ambient temperature.

By coupling these above results with XRD/SEM characterization conducted on the powders simultaneously withdrawn from the liquid medium, it can be deduced that the precipitation of the Mn-EG phase from the heated solution medium can be described as the overlapping of three reaction steps, the overall result being the formation of the Mn-EG precursor phase through a dissolution/crystallization process. More specifically, the first step is found to be a reduction of Mn in the starting MnO_2 with insertion of cationic species (H, Li), the second is a dissolution of the reduced phases so obtained, and the third is finally the precipitation of the Mn-EG phase from the solution. A thorough study of the mechanism involved in the first step and a complete characterization of the resulting MnO_2 reduced phases, which is beyond the scope of this paper, will be presented elsewhere [14].

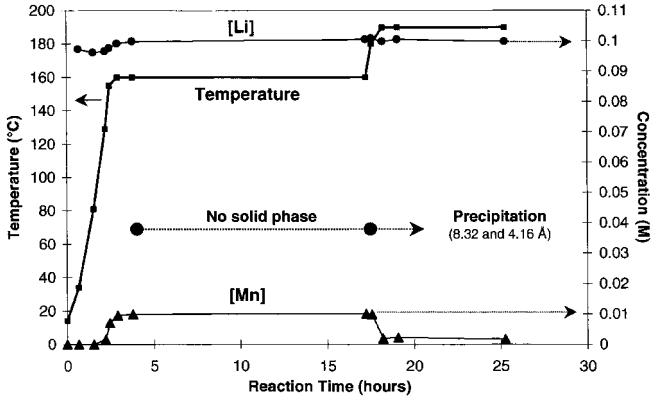

Fig. 7 Variation of the Li and Mn contents in the liquid organic phase as a function of the temperature and reacting time of LiOH and EMD in EG

The manganese oxidation state was measured in the final Mn-EG compound (2.10) and compared to that of the initial γ-MnO_2 (3.94). This finding confirms that EG acts as a reducing agent towards manganese and explains the color change (black $Mn^{4+} \rightarrow$ brown $Mn^{3+} \rightarrow$ pink Mn^{2+}) observed during the precipitation reaction. The reducing role played by the ethylene glycol medium was further indirectly demonstrated by performing an experiment using the same experimental conditions as stated above, but in water instead of EG medium. In that case no reaction did occur, as evidenced by the Mn o.s., IR spectrum and XRD pattern of the recovered black powder, which were similar to those of the initial EMD. Finally, since EG acts as a reducing agent, one would expect to find some oxidized product of EG in the reaction medium. Numerous products of EG degradation/oxidation (e.g. acetaldehyde, diacetyl) were indeed previously reported in other chemical reactions where EG was used as a reducing agent, e.g. in the preparation of metallic powders in EG medium [15].

The influence of the alkali hydroxide on the final Mn-EG precursor phase was also investigated. The experiments previously described using an ethylene glycol medium were conducted with the only difference being the nature of the hydroxide MOH. Besides LiOH, different hydroxides (KOH, NaOH) were tested. We found that the resulting Mn-EG precursors are independent of the nature of the alkali salt used during the dissolution/crystallization reaction. This simply means that the nature of the hydroxides used has no influence whatsoever on the final product of the reaction. A highly basic medium seems to be the only necessary condition for rapidly promoting the Mn dissolution in the EG solution from which the Mn-EG precursor phase precipitated. Indeed, we found that the Mn-EG phase can also be easily synthesized using ammonia instead of alkali hydroxides.

Li-polyol

Synthesis and characterization. Typically, 1–2 g of LiOH are treated at 160 °C in 100 ml of EG for a 2-h period. The resulting suspension is cooled down to room temperature and filtered. To the recovered yellow-orange liquid we add acetone under vigorous stirring until a white precipitate appears. The solid and liquid phases are separated by vacuum filtration and the obtained

product is washed with acetone, dried at 55 °C for 1 h and kept in moisture-free air. Indeed, this product is slightly hygroscopic and was found to transform in to lithium carbonate upon long periods of exposure to atmospheric moisture.

A typical XRD pattern of this powder is shown in Fig. 1b. A crystallographic parameters refinement leads to $a = 16.098(5)$ Å, $b = 8.072(2)$ Å and c = 5.035(2) Å in an orthorhombic cell. The IR spectrum of this phase shows characteristic absorption bands of an organic compound. The burning off of this organic compound from our precursor occurs around 200 °C, as shown on the DSC/TGA curves (Fig. 6b). The TGA product after ramping to 600 °C is identified as pure well-crystallized Li_2CO_3, and the calculation made from the weight loss (100–600 °C) leads to a Li content of 10.48% in the organometallic phase. This value is confirmed by AA measurements and is in perfect agreement with a proposed formula $Li(OCH_2CH_2OH)_1$ corresponding to a theoretical Li content of 10.21%. The presence of EG in this Li-EG phase is confirmed by infrared and NMR spectroscopy after dissolution of the powder in pure water (IR) and in D_2O (NMR). Both methods support the assumptions that (1) EG is present in the Li-EG product, and (2) no drastic transformation nor condensation of EG occurs during the synthesis. Furthermore, no trace of acetone, which could result from the precipitation/washing steps, could be found either by IR or by NMR. Finally, it should be noted that by adding another non-polar solvent besides acetone, miscible with EG, such as dimethylformamide (DMF) or acetonitrile, we also obtained precipitates showing the same composition, XRD pattern and IR spectrum as those of Li-EG precipitated with acetone. Only slight differences in the precipitation rates and in the Bragg peaks intensities of the resulting products were observed as a function of the solvents used. This result is difficult to account for since it indicates that the added solvent does not act as a reagent in the precipitation process, raising the still unanswered question. What is the true role of the solvent? The resulting precipitate was characterized by its specific surface area and morphology. A BET surface area of 19.3 m^2/g was measured on an Li-EG sample consisting of shapeless large and porous particles (as determined by SEM).

Spinel synthesis

On the basis of the Li and Mn contents previously calculated for Li-EG and Mn-EG, respectively, a stoichiometric (Li/Mn = 0.5) mixture of these two precursor phases is briefly ground in a mortar and heated under air using the following three-step heating sequence. First, a low heating rate (10°/h) from 25 °C to 250 °C with 10 h at 250 °C, followed by a faster heating rate (1°/min) from 250 °C to 800 °C, this final temperature being maintained for a 24-h period. Finally, the temperature is decreased down to room temperature at 1°/min. The first low heating step is necessary to avoid a too violent combustion, resulting in a loss of lithium (red flame). XRD showed that the final 800 °C product is a pure $LiMn_2O_4$ cubic phase (cell parameter $a = 8.244$ Å) that appears as expanded powder. By SEM, we observed that the platelet morphology of the initial Mn-EG phase is globally retained although particles are broken and sintered (Fig. 8a). This morphology is in total contrast with the polyhedral particles of the HT-$LiMn_2O_4$ powders made by the classical ceramic process (Fig. 8b). AA confirms that the initial Li/Mn atomic ratio is maintained after the heating treatment. By following the evolution of the XRD patterns as a function of the heating temperature, we observed that the spinel phase appears at temperatures as low as 250 °C, confirming that $Li_{1+y}Mn_{2-y}O_4$ formation is induced by the combustion of organic (e.g. autocombustion). This is also confirmed by IR, which shows the absence of the absorption bands characteristic of the organic within the product after treatment at 250 °C. It is important to note that at neither step of the heating process was a complete transformation towards $Mn_2O_3 + Li_2CO_3$

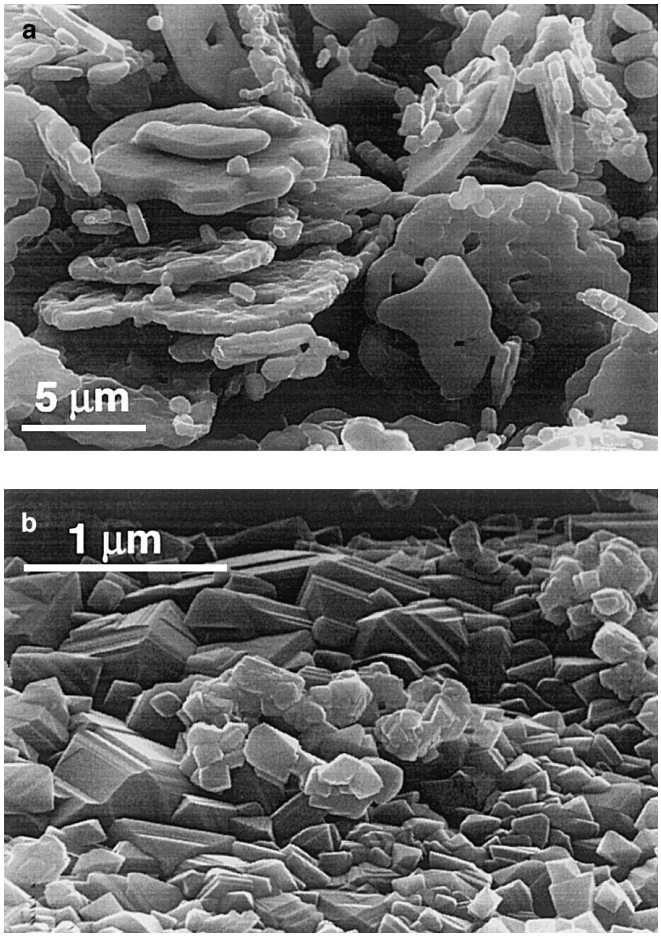

Fig. 8a, b SEM images showing the different morphologies of **a** $Li_{1+y}Mn_{2-y}O_4$ powder obtained by reacting a mixture of Li-EG/Mn-EG at 800 °C under air, and **b** $Li_{1+y}Mn_{2-y}O_4$ powder obtained by the classical ceramic route

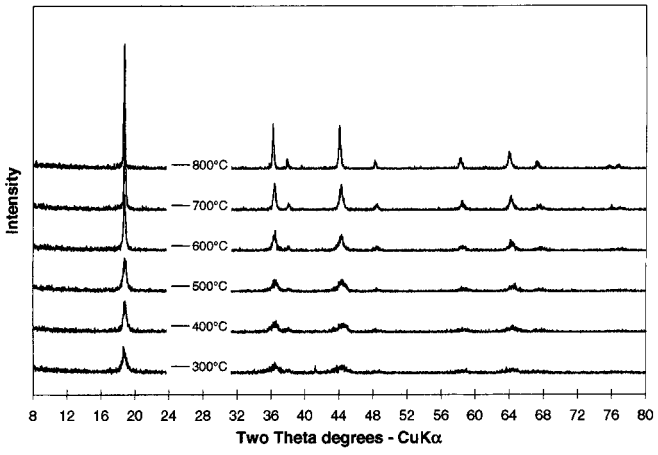

a

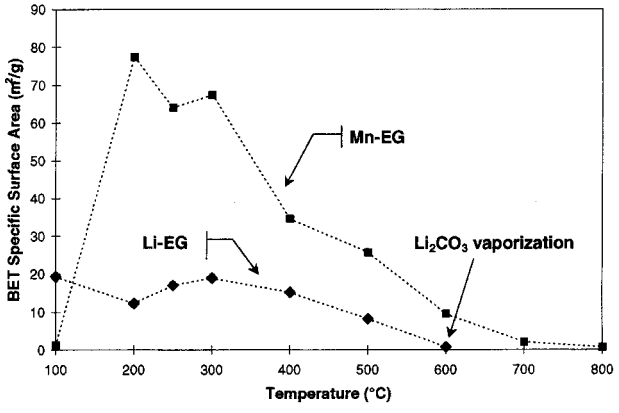

b

Fig. 9 **a** Evolution of the XRD pattern of $Li_{1+y}Mn_{2-y}O_4$ upon heating under air. **b** Evolution of the BET specific surface area versus annealing temperature of Li-EG and Mn-EG phases

observed, in contrast to other low-temperature routes reported. Finally, further heating at higher temperatures only increases the degree of crystallization of the powders, as exemplified in Fig. 9a, showing narrower Bragg reflections while the annealing temperature increases. The conservation of the global platelets shape from the Mn-EG to the spinel phase proves that the formation of the ternary oxide arises rather from a diffusion of the lithium within the Mn-O structure and cannot be described as a complete melting of both Li- and Mn-based precursors. Occasionally, for preparations from poorly mixed powders, a small amount of lithium carbonate is detected on material heated at low temperature, which disappears upon treatment at higher temperatures. The porosity of the spinel powders observed by SEM is most likely created during the burning of the organic component. The specific surface area changes of the precursor phases upon heating was determined by BET measurements. For such a measurement, two large batches of Li-EG and Mn-EG were separated into equal parts, each of which was heat treated under air at different temperatures in the 100–800 °C range following the three-step process described above. We found that the combustion of Li-EG (around 200 °C) is not associated with drastic BET surface area changes if compared to that of Mn-EG, which shows an important rise (2 $m^2/g \rightarrow 77$ m^2/g) at the firing temperature (Fig. 9b), and then decreases with higher post-annealing temperatures. The final specific surface value for the $Li_{1+y}Mn_{2-y}O_4$ powder obtained by this method is around 1 m^2/g, this value being similar to that obtained by the classical solid state reaction. This indicates that our synthesis method allows us to prepare $Li_{1+y}Mn_{2-y}O_4$ powders of similar specific surface area to that obtained by the ceramic method, but having a completely different morphology (platelet instead of cubic-shape particles).

Electrochemical tests

To test the electrochemical performance of these materials, we chose the spinel having the formula $Li_{1.05}Mn_{1.95}O_4$ made by the above method. As well as AA analyses, this y value (0.05) was indirectly confirmed by the value of the a cell parameter (8.225 Å), which was in good agreement with that reported by other authors [2] for an HT-made spinel of the same composition. $Li_{1.05}Mn_{1.95}O_4$/electrolyte/Li Swagelok cells were cycled at 25 °C and at 55 °C between 3.5 V and 4.8 V at C/5 current rate. At 25 °C, we noted that this material exhibited an irreversible capacity of $\Delta x = 0.05$ (Fig. 10a), while an irreversible capacity of $\Delta x = 0.07$ was measured under similar conditions for the ceramic-made materials. The fading capacity (Fig. 10b) upon cycling at 25 °C (7.7% after 200 cycles) favorably compares with that measured for the ceramic-made HT-$Li_{1.05}Mn_{1.95}O_4$ (10.4% after 200 cycles) under similar conditions. The first charge capacity for our $Li_{1.05}Mn_{1.95}O_4$ is evaluated from the voltage composition curve to be 124 mAh/g. This value is in perfect agreement with the theoritical capacity ($C = 126$ mAh/g) deduced from the general formula: C (mAh/g) $= (1-3y)$ 148 [16], where y is the value in $Li_{1+y}Mn_{2-y}O_4$. Upon cycling at 55 °C (Fig. 10c), we found that the capacity fading is larger than that measured at 25 °C and reaches 15% after 100 cycles. Again, this value is of the same order as that measured for our ceramic-made sample. Li-ion cells using these newly synthesized $Li_{1+y}Mn_{2-y}O_4$ powders have been made, and are presently being tested for their self-discharge performance at 55 °C. This will be reported in a forthcoming paper.

Conclusion

This work demonstrates that solution techniques can be used to prepare multi-component oxides of desired morphology and particle size if one selects the right precursors and defines the appropriate sintering behavior to preserve the precursor morphology. To obtain

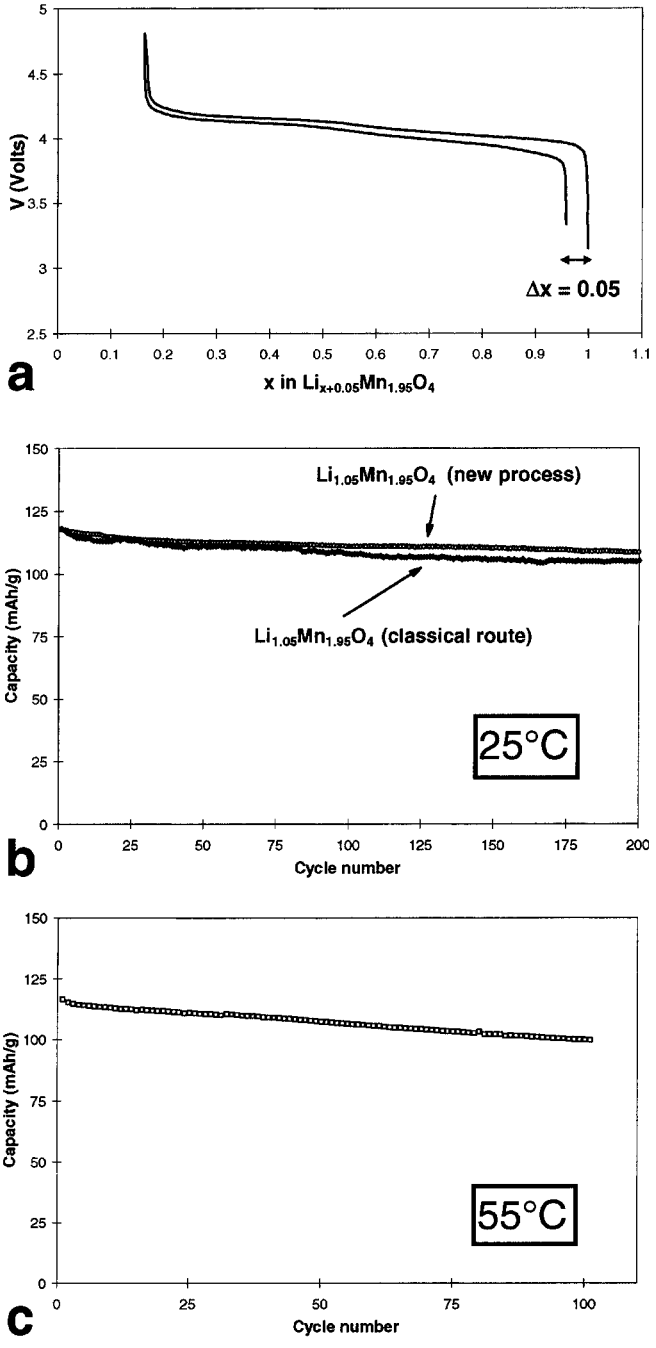

Fig. 10a–c Electrochemical characterization of $Li_{1.05}Mn_{1.95}O_4$ powder made by the new process: **a** galvanostatic first cycle curve, **b** variation of the capacity upon cycling at 25 °C, and **c** variation of the capacity upon cycling at 55 °C

electrochemically optimized $Li_{1+y}Mn_{2-y}O_4$ powders by the ceramic route, it was shown that intermittent grindings, a long annealing time at a temperature of 800 °C and, more importantly, a slow cooling step are required to ensure good atomic mixing, particle coarsening and maximum oxygen content, respectively [2]. We have demonstrated that the synthesis of $Li_{1+y}Mn_{2-y}O_4$ powders from Mn- and Li-based precursor phases offers a cheap method of producing powders with desired morphology, particle size and specific surface area. Our approach allows us to reduce the grinding steps of the ceramic process and also to avoid the slow cooling step because of different morphologies favoring a rapid oxygen uptake. Indeed, the high porosity and puffy nature of the powders allow for their rapid oxygenation even when the sample is rapidly cooled. Some studies are in progress to directly precipitate in one step the Li-EG and Mn-EG phases. In this way, both precursors will be intimately mixed and the grinding step further reduced. Furthermore, this approach is not specific to the synthesis of Mn-based oxides, but can be applied to other 3d-metal (e.g. Fe) oxides as will be reported elsewhere. Finally, by varying the nature of the MOH alkali hydroxide and/or of the polyol used, some new highly reactive M-polyol and Mn-polyol precursors can be synthesized. This opens up new low temperature synthetic routes for the preparation of various ternary metal oxides of controlled morphology/surface area for other fields of application besides electrochemistry, such as magnetic recording technology and catalysis.

Acknowledgements The authors would like to thank L. Dupont, V. Pralong, O. Gaildrat, G.G. Amatucci and L. Seguin for their helpful discussions. We also thank F. Dujeancourt and P. Bault for infrared and NMR measurements and for sharing their knowledge of these techniques.

References

1. Nagaura T (1990) 4th Internat Rechargeable Battery Seminar, Deerfield Beach, Florida
2. Tarascon JM (1995) US Patent 5 425 932
3. Barboux P, Tarascon JM, Shokoohi FKJ Solid State Chem (1991) 94: 185
4. Tsumura T, Shimizu A, Inagaki M (1993) J Mater Chem 3(9): 995
5. Prabaharan RSS, Michael MS, Kumar TP, Mani A, Athinarayanaswamy K, Gangadharan (1995) J Mater Chem 5(7): 1035
6. Katz MJ, Clarke RC, Nye WF, (1956) Ana Chem 25(4): 507
7. Guyomard D, Tarascon JM (1993) US Patent 5 192 629
8. Brunauer S, Emmett PH, Teller EJ (1938) Am Chem Soc. 60: 309
9. Dupont L. et al. (to be published)
10. Bach S, Pereira-Ramos J.P, Baffier N, Messina R (1991) Electrochim Acta 36(10): 1595
11. Strobel P, Le Cras F, Rohs S, Pontonnier L (1996) Mater Res Bull 31(11): 1417
12. Tekaia-Elhsissen K, Delahaye-Vidal A, Nowogrocki G, Figlarz M (1989) CR Acad Sci Paris 309 (II): 349
13. Tekaia-Elhsissen K, Delahaye-Vidal A, Nowogrocki G, Figlarz M (1989) CR Acad Sci Paris 309 (II): 469
14. Larcher D, Gérand B, Tarascon JM (to be published)
15. Blin B, Fievet F, Beaupère D, Figlarz M (1989) New J Chem 13: 67
16. Gummow RJ, Kock A de, Thackeray MM (1994) Solid State Ionics 69: 59